

## Hierarchical noise in large systems of independent agents

Claus Wilke and Thomas Martinetz

*Institut für Neuroinformatik, Ruhr-Universität Bochum, D-44780 Bochum, Germany*

(Received 22 May 1998)

A generalization of the coherent-noise models [M. E. J. Newman and K. Sneppen, *Phys. Rev. E* **54**, 6226 (1996)] is presented where the agents in the model are subjected to a multitude of stresses, generated in a hierarchy of different contexts. The hierarchy is realized as a Cayley tree. Two different ways of stress propagation in the tree are considered. In both cases, coherence arises in large subsystems of the tree. Clear similarities between the behavior of the tree model and of the coherent-noise model can be observed. For one of the two methods of stress propagation, the behavior of the tree model can be approximated very well by an ensemble of coherent-noise models, where the sizes  $k$  of the systems in the ensemble scale as  $k^{-2}$ . The results are found to be independent of the tree's structure for a large class of reasonable choices. Additionally, it is found that power-law distributed lifetimes of agents arise even under the complete absence of correlations between the stresses the agents feel. [S1063-651X(98)09012-6]

PACS number(s): 05.90.+m, 87.10.+e

### I. INTRODUCTION

It has recently been shown that in large systems of independent “agents,” the interplay of two different types of noise can lead to power-law distributed quantities, such as lifetimes of the agents or sizes of reorganization events [1]. One of the two noises, usually referred to as stress, has to act coherently on all agents, while the other one, usually referred to as mutation or reloading, has to act individually on each agent, and on a much longer time scale. Mechanisms of this kind have been called “coherent-noise” mechanisms. Models incorporating coherent-noise mechanisms have been put forward to explain effects seen in earthquakes, rice piles, or biological evolution and extinction [1–4].

In most applications, however, it is hard to justify a single stress imposed on the whole system at once. In Ref. [2], the stress was identified with global influences on the biosphere, as in the case of extraterrestrial impacts [5]. Nevertheless, there are more reasons for species to go extinct than impacts. Often, species' extinction is a local phenomenon [6]. For example, species living in a small territory regularly die out because of the invasion of a new species, able to exploit their ecological niche more effectively. A similar argument applies to the situation of earthquakes. In Ref. [1] the stress has been interpreted as background noise with long wavelength, generated by some distant external source. Nonetheless, in a large fault system, we would expect background noise to be present also locally, and probably on smaller and larger scales at the same time [7].

The aim of the present paper is to advance a model that, while incorporating the basic ideas of coherent-noise systems, can deal with more complex situations by considering stress on different scales. A short account of this work has already been given elsewhere [8]. There, only regular trees (see below) have been treated.

### II. AGENTS IN A HIERARCHICAL CONTEXT

It is an observation from everyday life, as well as from many physical systems [9], that very often objects or agents

are embedded into a hierarchy of different contexts, all having influences on them. Mathematically, this idea can be described with the concept of ultrametricity [10], which means there exists a distance  $d(\cdot)$  such that the triangle inequality  $d(A_1, A_3) \leq \max\{d(A_1, A_2), d(A_2, A_3)\}$  holds for any three agents  $A_1, A_2, A_3$ . Geometrically, an ultrametric space can be conceived of as a Cayley tree. In the following, vertices in the tree connected to exactly one other vertex will be called leaves, and vertices connected to two or more other vertices will be called nodes. In this paper, the nodes of the tree stand for different contexts, and the agents are placed at the tree's leaves.

We can formulate a generalization of the original coherent-noise model by incorporating the above ideas. Our system consists of  $N$  agents, each represented by a real number (threshold)  $x_i$  or, in the general case, a vector  $\mathbf{x}_i$ . Furthermore, we choose a tree with  $N_n$  nodes and  $N_l = N$  leaves, which means  $N_v = N_n + N_l$  vertices in total. The tree will be kept fixed throughout the simulation. At every leaf we put exactly one agent. For every node  $j$  of the tree we choose a stress distribution with probability density function (PDF)  $p_j(x)$ . Additionally, we also choose a stress distribution for every leaf of the tree, so that we have a stress distribution for every vertex of the tree. The stress distributions at the leaves allow us to simulate extremely localized influences acting on only a single agent. The total number of stresses in the system is therefore  $N_{\text{stress}} = N_v$ .

The course of the simulation runs as follows. At the beginning, the agents are initialized with random thresholds drawn from a distribution  $p_{\text{thresh}}(x)$ . Then, in every time step, three actions are performed. (i) From each of the  $N_{\text{stress}}$  stress distributions, a stress  $\eta_j$  is chosen at random. (ii) For every agent  $i$ , from all the  $S_i$  stress values  $\eta_1^{(i)}, \dots, \eta_{S_i}^{(i)}$  above the agent in the tree, a stress  $\eta_i^{\text{eff}}$  is calculated according to some function  $\mathcal{A}$ :

$$\eta_i^{\text{eff}} = \mathcal{A}(\eta_1^{(i)}, \dots, \eta_{S_i}^{(i)}). \quad (1)$$

If  $\eta_i^{\text{eff}} \geq x_i$ , agent  $i$  is removed and replaced by a new one

with a threshold chosen at random from  $p_{\text{thresh}}(x)$ . (iii) Finally, every agent has a small probability  $f$  to get a new threshold, again from the distribution  $p_{\text{thresh}}(x)$ . Action (iii) represents the mutation or reloading mentioned in the Introduction.

There are a number of reasonable choices for the function  $\mathcal{A}$ . In this paper, we will mainly study the ‘‘maximum rule,’’ which reads

$$\mathcal{A}(\eta_1^{(i)}, \dots, \eta_{S_i}^{(i)}) = \max\{\eta_1^{(i)}, \dots, \eta_{S_i}^{(i)}\}. \quad (2)$$

Another natural choice is to sum up the stresses, i.e., to use

$$\mathcal{A}(\eta_1^{(i)}, \dots, \eta_{S_i}^{(i)}) = \sum_{j=1}^{S_i} \eta_j^{(i)}. \quad (3)$$

This alternative, which we will call ‘‘sum rule,’’ will also be discussed in this paper.

### III. THE EFFECTIVE STRESS DISTRIBUTION

The effective stress an agent feels can be calculated exactly in the case of the maximum rule, Eq. (2). The agent is subjected to the stress distribution at its leaf and to the stress distributions at the nodes above it. Let there be  $S-1$  nodes above the leaf of an agent. Then the  $S$  stress values having influence on this agent are  $S$  random variables  $X_1, \dots, X_S$  with PDF's  $p_1(x), \dots, p_S(x)$ . To obtain the effective stress distribution, we have to calculate the PDF  $p_{\text{max}}(x)$  of the random variable  $X_{\text{max}} = \max\{X_1, \dots, X_S\}$ , i.e.,

$$p_{\text{max}}(x) dx = P(x \leq \max\{X_1, \dots, X_S\} < x + dx). \quad (4)$$

Note that

$$P(\max\{X_1, \dots, X_S\} \leq x) = \prod_i^S P(X_i \leq x). \quad (5)$$

The derivative of Eq. (5) with respect to  $x$  yields

$$p_{\text{max}}(x) = \sum_{i=1}^S p_i(x) \prod_{j=1, j \neq i}^S P(x > X_j). \quad (6)$$

Equation (6) is the exact expression for the effective stress on an agent in the case of the maximum rule, Eq. (2). A simple calculation shows that the right-hand side of Eq. (6) is dominated by the slowest decaying stress distribution. We say that a distribution  $p_i(x)$  decays slower than another distribution  $p_j(x)$  if there exists a  $x_0$  such that

$$p_i(x) > p_j(x) \text{ for all } x > x_0. \quad (7)$$

For a set of reasonable stress distributions it is always possible to identify the distribution  $p_0(x)$  that is falling off slowest according to this definition. Hence, we find for the PDF of the effective stress on an agent

$$p_{\text{max}}(x) \sim p_0(x) \text{ for } x \rightarrow \infty. \quad (8)$$

A similar statement cannot easily be proved for the sum rule. However, in special cases the necessary calculations

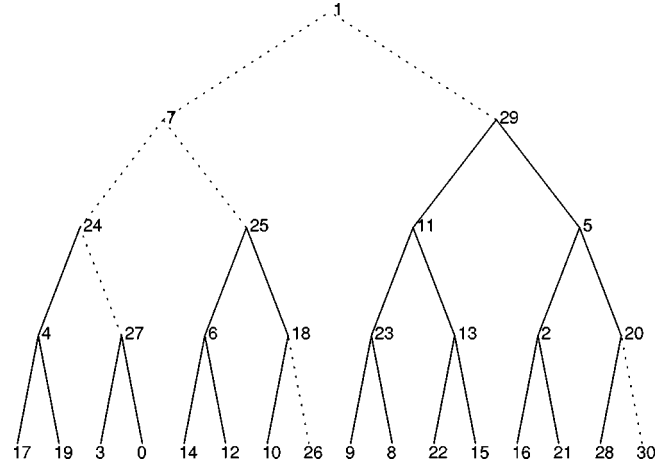


FIG. 1. The breakdown of a regular tree with  $n=2$  and  $l=4$  into independent subsystems. The solid lines connect agents with the same rank, the dashed lines connect agents with different ranks. In this example, we have two subsystems of size 1 (ranks 26 and 30), two of size 2 (ranks 24 and 27), one of size 3 (rank 25), and one of size 7 (rank 29).

can be done. Consider, for example, the case of exponential stress distributions  $p_i(x) = \exp(-x/\sigma_i)/\sigma_i$ . In this case, we find

$$p_{\text{sum}}(x) \sim \frac{1}{\sigma_{\text{max}}} \exp\left(-\frac{x}{\sigma_{\text{max}}}\right) \text{ for } x \rightarrow \infty, \quad (9)$$

where  $\sigma_{\text{max}} = \max\{\sigma_1, \sigma_2, \dots, \sigma_n\}$ . A similar result can be found in the case of stress distributions with power-law tails [8]. It seems that in most of the reasonable cases, the sum of the stresses will be dominated by a single distribution in the limit of large stresses, as in the situation of the maximum of the stresses.

### IV. REGULAR TREES

In this section we are interested in trees which are constructed as follows. We begin with a single leaf and convert it into a node by connecting to it  $n$  new leaves. Then we repeat this procedure for every new leaf. We stop the construction when we have reached a depth of  $l$  iterations. Trees generated in this way are called regular trees [11]. The tree displayed in Fig. 1 is a regular tree with  $n=2$  and  $l=4$ .

The number of leaves in a regular tree is

$$N_l = n^l, \quad (10)$$

and the number of vertices is

$$N_v = \sum_{i=0}^{l-1} n^i. \quad (11)$$

Therefore, we have  $N=n^l$  agents in such a tree, and  $N_v$  stress values have to be generated in every time step.

We saw in Sec. III that every agent feels effectively a single stress distribution in the limit of large stresses [Eqs. (8),(9)]. Since for coherent-noise systems, large stresses give the main contribution to the systems' behavior, the stress distributions that are falling off very slowly dominate large

parts of the tree. Hence, the tree breaks down into subsystems that are to some extent decoupled from each other. For regular trees, it is relatively easy to study the average distribution of the subsystems' sizes analytically. We assume for any two stress distributions  $p_i(x), p_j(x)$  in the tree we can identify one of the two that is falling off slower, according to Eq. (7). This is not a severe restriction, as we have noted in Sec. III. Additionally, we restrict ourselves to situations in which  $p_i(x)$  and  $p_j(x)$  are equally likely to fall off slower than the respective other. Under these conditions, we can rank all stress distributions in a tree, assigning rank 1 to the one that is falling off fastest, and assigning correspondingly higher ranks to the ones that are falling off slower. This makes the calculation of the subsystems' sizes relatively easy. For every single agent, we have to identify the corresponding highest rank placed above it in the tree (which we will call the rank of the agent). Then, we simply have to count the number of agents with the same rank. This procedure is illustrated in Fig. 1.

We expect the mean distribution of subsystems' sizes to have sharp peaks whenever the size of a complete subtree is reached, because the probability for a single rank to be higher than all others further down the tree should be larger than the probability for a complicated arrangement of ranks to produce a subsystem of a certain size. The size  $k$  of a subsystem is the number of leaves in that subsystem. The functional dependency of the peaks at size  $k$  is calculated as follows. The expected frequency  $f(k)$  of independent subtrees of depth  $b$ , corresponding to a subsystem of size  $k = n^b$ , can be written as the number of such subtrees in the whole system  $N_{\text{sub}}(n^b)$  times the probability that any of these subtrees will be independent of the rest  $P_{\text{indep}}(n^b)$ . Hence we write

$$f(n^b) = N_{\text{sub}}(n^b) P_{\text{indep}}(n^b). \quad (12)$$

The number of subtrees of size  $n^b$  is

$$N_{\text{sub}}(n^b) = n^{l-b}. \quad (13)$$

A subtree is independent of the rest if the rank at its root is higher than all other ranks in the subtree and at the nodes above the subtree. The probability  $P_{\text{indep}}(n^b)$  is therefore the reciprocal of the number of vertices in the subtree plus the number of vertices above the subtree, hence,

$$P_{\text{indep}}(n^b) = \left( l - b + \sum_{i=0}^b n^i \right)^{-1}. \quad (14)$$

If we increase  $b$  by one, we get  $N_{\text{sub}}(n^{b+1}) = n^{l-b-1} = N_{\text{sub}}(n^b)/n$ . With slightly more effort, we find also

$$\begin{aligned} P_{\text{indep}}(n^{b+1}) &= \left( l - b - 1 + \sum_{i=0}^{b+1} n^i \right)^{-1} \\ &= \left( l - b + n \sum_{i=0}^b n^i \right)^{-1} \approx \frac{1}{n} P_{\text{indep}}(n^b). \end{aligned} \quad (15)$$

Therefore, we can write

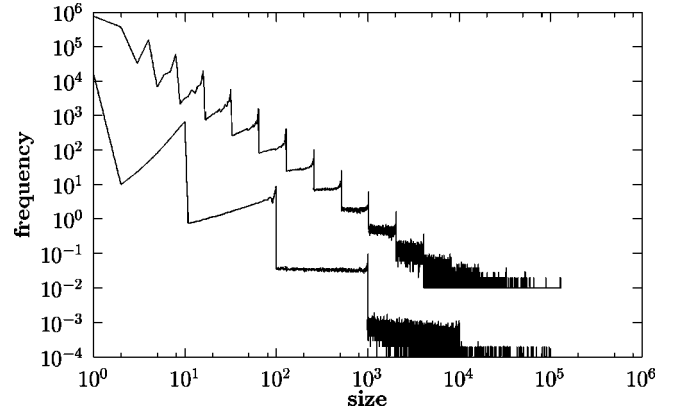


FIG. 2. The expected frequency of subsystems of size  $k$  decreases as a sawtooth function following approximately a power law with exponent  $-2$ . The upper curve stems from a tree with  $l = 17$  and  $n = 2$ . It has been rescaled by a factor of 100 so as not to overlap with the lower curve. The lower curve stems from a tree with  $l = 5$  and  $n = 10$ . Quantities are plotted in arbitrary units.

$$f(nk) \approx \frac{N_{\text{sub}}(nk)}{n} \frac{P_{\text{indep}}(nk)}{n} = n^{-2} f(k), \quad (16)$$

which implies  $f(k) \sim k^{-2}$ .

This result is interesting. The frequency of subsystems of size  $k$  scales as  $k^{-2}$ , independent of the parameter  $n$  which characterizes the structure of the tree.

We have tested these predictions by measuring the frequency  $f(k)$  in computer experiments. Our simulations are set up as follows. We choose a tree with  $N_v$  vertices in total. For several thousand times, we assign the integers from 1 to  $N_v$  randomly to the vertices of the tree. The integers stand for the rank of the stress distributions at the vertices. For every single realization of this process, we determine the sizes of the subsystems the tree breaks down into, and compute a histogram of the sizes' frequencies. Finally, we calculate the average over all histograms.

Figure 2 shows the results of such measurements for two different trees with 10 000 histograms each. We can see clear peaks at powers of  $n$ , which correspond to complete subtrees. We also find the heights of the peaks to decrease as  $k^{-2}$ , in agreement with Eq. (16).

## V. RANDOM TREES

The regular trees treated in the previous section can be easily generalized to a broader class of trees, which we will call "random trees." Only a small change in the construction algorithm is necessary. To construct a regular tree, in every iteration step we connect  $n$  new leaves to every leaf of the previous step. The straightforward generalization of this procedure is to choose a random number of new leaves for every leaf of the previous construction step. To avoid confusion with the parameter  $n$ , we will call this random number  $n_{\text{rand}}$ . The random variable  $n_{\text{rand}}$  will take value  $i$  with probability  $p_i$ , i.e.,  $P(n_{\text{rand}} = i) = p_i$ ,  $i = 0, 1, 2, \dots$ ,  $\sum_i p_i = 1$ . We denote the mean of  $n_{\text{rand}}$  by  $m := \langle n_{\text{rand}} \rangle$  and the variance by  $\sigma^2$ . Moreover, we assume  $m > 1$  in all cases considered in this paper. In the limit  $\sigma^2 \rightarrow 0$ , the random trees reduce to regular trees with  $n = m$ .

The construction of a random tree as prescribed above is a branching process with  $l$  generations. From the theory of branching processes [12], we know that for large  $l$  the number of leaves in the tree will be

$$N_l = Wm^l, \quad (17)$$

where  $W$  is a random variable with mean  $\langle W \rangle = 1$ . The factor  $W$  takes into account fluctuations that happen at the beginning of the tree's construction. Correspondingly, for the total number of vertices in the tree we use the approximation

$$N_v \approx W \sum_{i=0}^l m^i. \quad (18)$$

The above two equations are the generalizations of Eqs. (10),(11) for random trees.

As in the case of regular trees, we are interested in the quantity  $f(k)$ , the expected frequency with which independent subsystems of size  $k$  occur. In the previous section we made the assumption that the main contributions to  $f(k)$  come from complete subtrees. The comparison with numerical data showed that this assumption leads to a good understanding of the structure of  $f(k)$ . Consequently, in the case of random trees we also assume that we can concentrate on complete subtrees.

The number of subtrees of size  $k$  in a large tree is on average the size of the tree (which is the number of leaves in the tree) divided by  $k$ . Hence we have

$$N_{\text{sub}}(k) = \frac{N_l}{k}, \quad (19)$$

which is equivalent to Eq. (13) for regular trees.

The probability for a subtree of size  $k$  to be dominated by a single stress distribution is one over the total number of vertices in the subtree. The number of vertices is asymptotically the same as the number of leaves. This can be seen from Eqs. (17) and (18). The leading term in the number of vertices in a random tree Eq. (18) is exactly the expression for the number of leaves in the same tree Eq. (17). Hence we have

$$P_{\text{indep}}(k) \sim \frac{1}{k}. \quad (20)$$

We combine this result with Eq. (19) and obtain

$$f(k) \sim \frac{1}{k^2}. \quad (21)$$

As in the case of regular trees, the frequency of independent subtrees of size  $k$  scales as  $k^{-2}$ , independent of the details of the tree. With a little effort, it is also possible to calculate the constant of proportionality. We find

$$f(k) = \frac{\alpha N_l}{k^2} \frac{m-1}{m}, \quad (22)$$

with

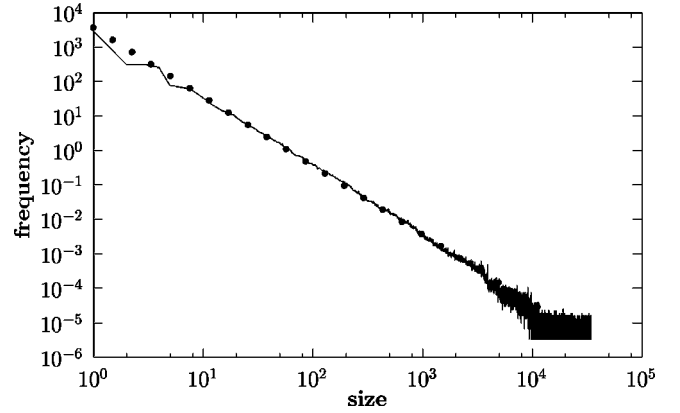


FIG. 3. The expected frequency of subsystems of size  $k$  in a random tree with  $m = 1.993$  and  $l = 13$ . The dotted line is the approximation Eq. (22). Quantities are plotted in arbitrary units.

$$\alpha = \left[ \sum_{k=1}^{N_l} \frac{1}{l+1 - \log_m k + (k-1)[m/(m-1)]} \right]^{-1}. \quad (23)$$

Equation (22) is in good agreement with measurements from computer experiments. We have done simulations with several different probability distributions for  $n_{\text{rand}}$ , such as uniform [ $p_0 = c/(n_{\text{max}} + c)$ ,  $c \geq 0$ ,  $p_i = 1/(n_{\text{max}} + c)$  for  $1 \leq i \leq n_{\text{max}}$ ,  $p_i = 0$  for  $n_{\text{max}} < i$ ], geometric series [ $p_i = bc^{i-1}$  for  $i \geq 1$ ,  $b, c > 0$ ,  $b \leq 1 - c$ ,  $p_0 = 1 - \sum_{j=1}^{\infty} p_j$ ], or Gaussian ( $p_i \sim \exp[-(i-b)^2/c]$ ; here  $b$  and  $c$  are not mean and variance, because we use only discrete values of the Gaussian probability density function). In all cases, we find Eq. (22) to approximate well the measured frequency  $f(k)$ . An example is shown in Fig. 3. Deviations from the straight line can be seen for very small  $k$  and for very large  $k$ . In these two limiting cases, the assumptions of the above approximations are no longer valid. Consider first the case of a very small  $k$ . This corresponds to  $k \approx m$ , because we always assume  $m \ll N_v$  (otherwise, the tree would have roughly a depth of 1, which would not be very interesting). If  $k$  is close to  $m$ , the number of subtrees of size  $k$  depends strongly on the exact form of the probability distribution of  $n_{\text{rand}}$ , and Eq. (19) is no longer valid. Since, as seen above, the main contribution to  $f(k)$  comes from complete subtrees, the distribution of  $n_{\text{rand}}$  then has effects on  $f(k)$ . For example, in a situation where  $P(n_{\text{rand}} = m) = 0$ , there should be a clear dip in  $f(k)$  at  $k = m$ .

Consider now the case of a very large  $k$ . Again Eq. (19) is no longer valid. This time because there are so few subtrees of size  $k$ . Hence, the exact structure of the tree comes into play. For example, a tree with  $N_v = 10^5$  containing a subtree with  $k = 6 \times 10^4$  will not contain another subtree with  $k = 5 \times 10^4$ . Therefore, in this situation there should be a clear peak at  $k = 6 \times 10^4$ .

## VI. SIMULATION RESULTS

As the main result of Secs. IV and V, we found the distribution of independent subsystems of size  $k$  in the tree to be proportional to  $k^{-2}$ . Therefore, in the limit of large stress values  $\eta$ , we expect the tree model to behave like an ensemble of coherent-noise models whose sizes scale as  $k^{-2}$ .

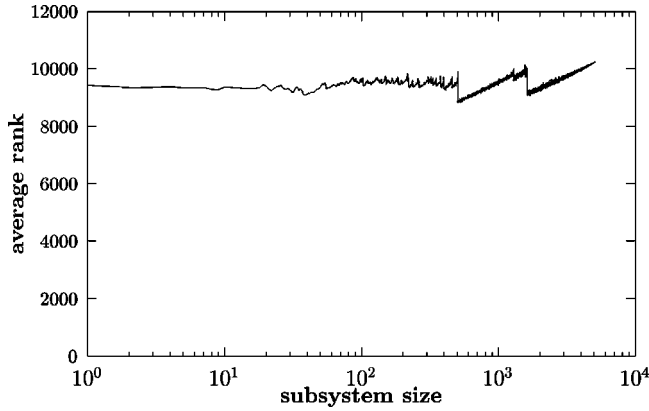


FIG. 4. The average rank of the subsystems in a random tree. Quantities plotted are dimensionless.

When constructing the ensemble approximation of a certain tree, we have to choose the right stress distribution for every coherent-noise model in the ensemble. In principle, this can be a complicated task. However, we have found that a very simple approach instead works sufficiently well in many cases. It can be motivated with Fig. 4. There, we have recorded the average ranks of the subsystems in a tree. Interestingly, the average rank varies only very little with the subsystem's size  $k$ . Therefore, in a further approximation, we assume that all the stress distributions that dominate a subsystem have the same rank, i.e., they are all the same (we use a single *stress distribution*, but the *stress values* are still chosen independently for all systems in the ensemble).

Our numerical simulations show the similarity between the tree model and the ensemble. We begin with results for the maximum rule.

#### A. The distribution of event sizes

As in previous work [13,14], an “event” is the reorganization of agents because of stress in a single time step. The size of an event is the total number of agents hit by the stress.

The event sizes of a typical simulation with maximum rule are recorded in Fig. 5. The lower curve shows the dis-

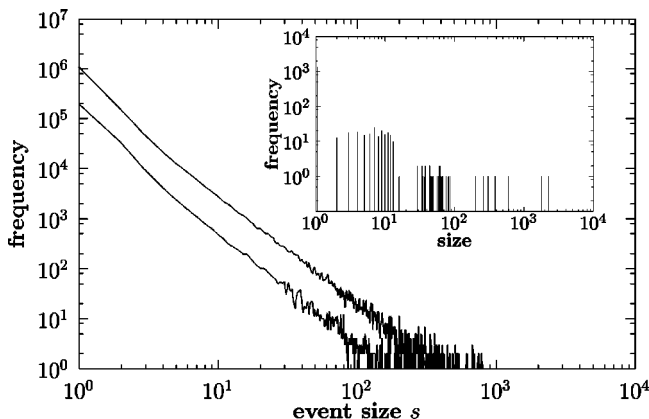


FIG. 5. The event size distribution in a random tree (lower curve) and in the corresponding ensemble of coherent-noise systems (upper curve). The inset shows the distribution of the tree's subsystems. Quantities are plotted in arbitrary units.

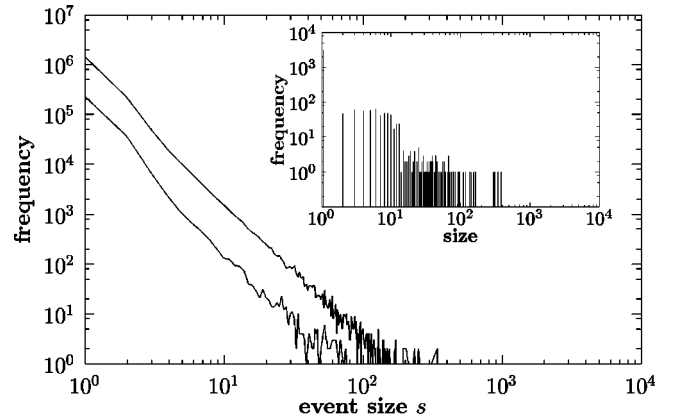


FIG. 6. The event size distribution in a random tree (lower curve) and in the corresponding ensemble of coherent-noise systems (upper curve). The structure of the tree is the same as in Fig. 5, but the stress distributions at the vertices are different. The inset shows again the distribution of subsystems obtained from the ranking procedure. Quantities are plotted in arbitrary units.

tribution of event sizes of a tree model, the upper curve shows the same distribution of the corresponding ensemble of coherent-noise systems. The heights of the curves reflect the total number of events we recorded for each model and have no special meaning. The sizes of the systems in the ensemble are exactly the ones we obtained for the sizes of the tree's subsystems while doing the ranking procedure described in Sec. IV. The distribution of these sizes is shown in the inset of Fig. 5.

The tree used in Fig. 5 is a random tree with 14 213 vertices and 12 163 leaves. Hence, both the tree model and the ensemble contain 12 163 agents in total. The stress distributions used in the tree are exponentials  $\exp(-x/\sigma_i)/\sigma_i$ , with different values  $\sigma_i$  between 0.03 and 0.06. The stress distribution used in the ensemble is an exponential with  $\sigma = 0.06$ .

As we can see in Fig. 5, the tree model and the ensemble behave very similar with regard to event sizes. In both cases, we find approximately a power-law decrease. A power-law fit gives an exponent of  $2.3 \pm 0.15$  for the tree model, and of  $2.2 \pm 0.15$  for the ensemble. Note the clear difference between the exponent in these two systems and the exponent in a single coherent-noise model with exponential stress. There, the exponent is  $1.85 \pm 0.03$  [13].

The event-size distribution depends strongly on the distribution of the subsystems in the tree. In Fig. 6, we have used the same tree structure and the same stress distributions as in Fig. 5, but the stress distributions have been assigned to different vertices. As a result, in this case the tree model has a lack of large subsystems, as can be seen in the inset of Fig. 6. Consequently, large events appear less frequently, and the distribution is significantly steeper than in Fig. 5 (now we have an exponent of  $2.9 \pm 0.2$  for the tree model and an exponent of  $2.8 \pm 0.2$  for the ensemble).

It would be interesting to average over all possible assignments of the stress distributions to the different vertices in order to gain a better understanding of a typical event size distribution in a large tree. However, we are not able to reach such a result due to the enormous amount of computing power that is needed. The simulation of the full tree as in

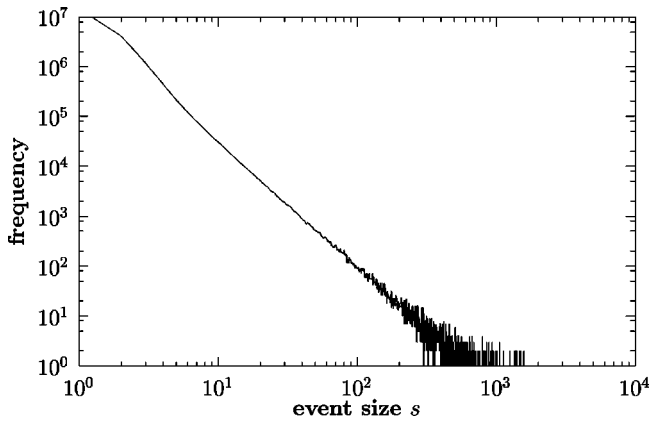


FIG. 7. Mean event size distribution of the ensemble approximation to a tree with 10 000 leaves. The average was taken over 60 randomly generated ensembles. Quantities are plotted in arbitrary units.

Figs. 5 or 6 takes in fact about 150 hours of computing time on a UltraSPARC 2 with 168 MHz. On the other hand, the simulation of the ensemble approximation takes only 6 hours on the same system. Therefore, we can do the corresponding calculations for the ensemble approximation. Of course we cannot average over all possible configurations, but we can average over a reasonably large random sample. We have generated 60 ensemble approximations of a tree with 10 000 leaves. The event size distributions we found were all very similar. In Fig. 7 we display the average event size distribution we obtained. The distribution has a power-law tail with exponent  $2.5 \pm 0.05$ .

### B. Aftershocks

Coherent-noise models display aftershocks [1,14], i.e., an increased number of large events can be observed in the aftermath of a very large event. Consequently, we study the decay pattern of the aftershocks in the tree model and in the ensemble. We will restrict ourselves to the case of events in the aftermath of an initial infinite event. We follow closely the ideas and methods developed in Ref. [14]. Figure 8 shows the change of the probability  $P_t(s \geq s_1)$  with time.  $P_t(s \geq s_1)$  is the probability to find an event larger than some constant  $s_1$  at time  $t$  after an initial infinite event. For both the tree model and the ensemble, the probability  $P_t(s \geq s_1)$  decreases with time, indicating aftershocks. However, we do not observe a clear power-law decrease, normally visible in the case of coherent-noise models [14].

As in the case of event sizes, we find a close similarity between the tree model and the ensemble. Let us first focus on the upper two curves in Fig. 8, which correspond to  $s_1 = 0.02$  and  $s_1 = 0.0025$  (here,  $s_1$  is measured in units of the number of agents in the tree, which was 12 163 in this case). For large  $t$ , the curves for the tree model and for the ensemble lie on top of each other, indicating the same decay pattern for long-time correlations. Only for small times there are some deviations between the two models. The tree model produces more aftershocks shortly after the infinite event. This observation has its origin in the fact that the two models converge in the limit of large stresses, but the number of moderate stresses produced by the tree model is significantly larger than the one produced by the ensemble. At short times

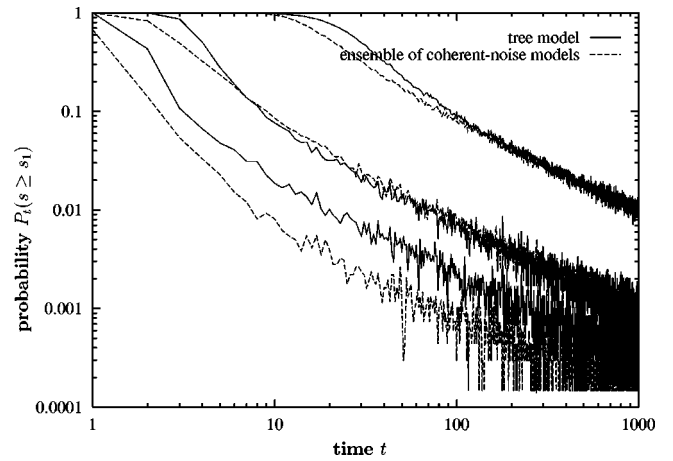


FIG. 8. The probability  $P_t(s \geq s_1)$ . The solid lines stem from the tree model, the dashed lines stem from the corresponding ensemble. From bottom to top, we have  $s_1 = 0.05$ ,  $s_1 = 0.02$ , and  $s_1 = 0.0025$ , where  $s_1$  is measured in units of the maximal system size. For the upper two curves, the results for the tree model are very close to the ones for the ensemble. The discrepancies in the lower curve are explained in detail in the text. Quantities plotted are dimensionless.

after a very large event, already moderate stresses can trigger large events, thus increasing the number of events seen in the tree model as compared to the ensemble.

For large values of  $s_1$ , the similarity between the two models seems to disappear. The curves in Fig. 8 corresponding to  $s_1 = 0.05$  do not lie on top of each other. The curve for the tree model is shifted upwards by about a factor of 3. This discrepancy for large  $s_1$  can be understood from Fig. 9. There, we display the frequency distribution of the events that have been produced during the simulations for Fig. 8. The results for the tree model and for the ensemble are very similar. However, at an event size of about 1000, the frequency distribution for the ensemble falls off rather quickly, whereas the frequency distribution for the tree has an additional peak at about 1400. It is this peak that causes the shift of the probability  $P_t(s \geq s_1)$  in the tree model for large  $s_1$ .

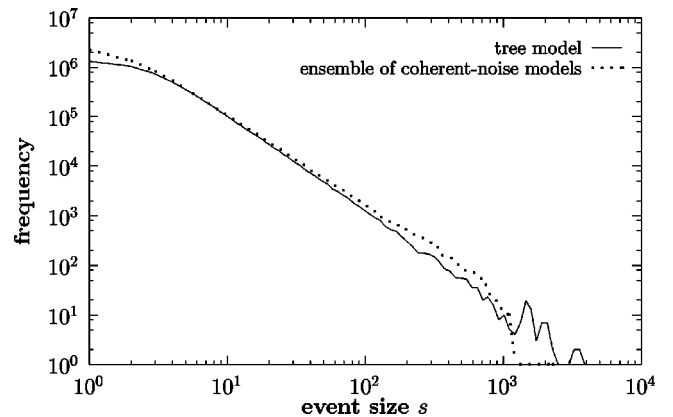


FIG. 9. A histogram of the event sizes that have been produced in the simulations for Fig. 8. Note that we recorded events only up to 1000 time steps after the infinite event. Therefore, the exponent of the power law is different from the one in Fig. 5. Quantities are plotted in arbitrary units.

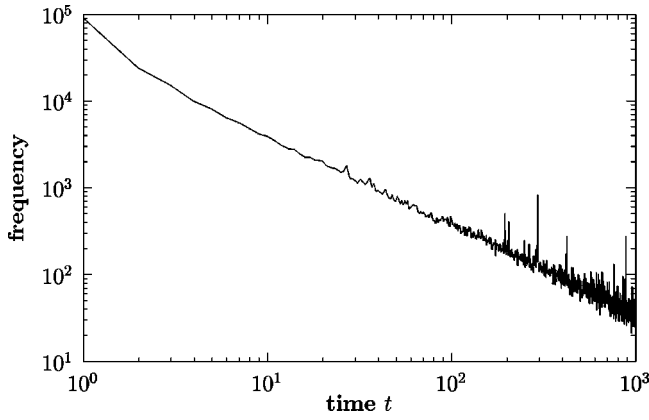


FIG. 10. The distribution of lifetimes in a random tree with exponential stresses only. We find a power-law with an exponent of  $-1.02$ . This is the same result as in a coherent-noise model with exponential stress. Quantities are plotted in arbitrary units.

The peak in the tree model arises because from time to time a very large stress will be generated at the root of the tree, causing an event of the order of the tree's size. In the ensemble, on the other hand, events larger than the largest subsystem are extremely unlikely.

### C. The distribution of lifetimes

The lifetime of an agent is the time an agent remains in the system without being hit by stress. In the original coherent-noise model, the agents' lifetimes are distributed as a power law with exponent  $2 - 1/\alpha$  [13]. The quantity  $\alpha$  depends on the stress distribution, and it is related to the mean-field exponent  $\tau$  of the event size distribution by  $\tau = 1 + \alpha$ . For exponential stress, e.g., we have  $\alpha = 1$ . Hence, in this case the lifetimes  $L$  are distributed as  $L^{-1}$ .

The distribution of lifetimes in a coherent-noise model does not change if the stress is imposed on each agent independently, instead of being imposed on all agents coherently. This is different to the case of event sizes or aftershocks. It can be seen as follows. The derivation of the lifetime distribution in Ref. [13] makes use of the time-averaged distribution of the agents' thresholds, which remains the same whether or not the stress is imposed coherently. The only further assumptions that enter the calculation are assumptions about the form of  $p_{\text{stress}}(x)$  and  $p_{\text{thresh}}(x)$ , but no assumptions about the coherence of stresses are made. Therefore, the distribution of lifetimes in a coherent-noise model and in a large ensemble of degenerate coherent-noise models with size 1 is the same, provided the stress distributions and the threshold distributions are the same. Consequently, if the stress-distributions in the tree have all the same  $\alpha$  (e.g., are all exponentials), the distribution of the agents' lifetimes should be similar to the one in a coherent-noise model with  $\tau = 1 + \alpha$ . This can be seen in Fig. 10. The distribution of lifetimes in a random tree with exponentially distributed stresses is similar to the one in a coherent-noise model with exponential stress (compare, e.g., Fig. 10 with Fig. 5 in Ref. [13]).

### D. Trees with sum rule

In the previous paragraphs, we studied simulations with the maximum rule. Here, we will present some results from

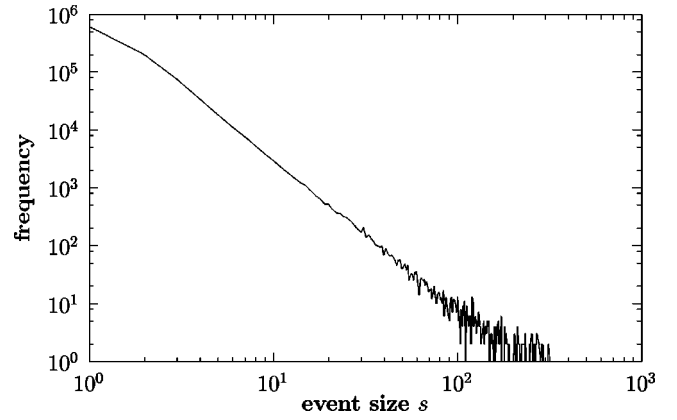


FIG. 11. The distribution of event sizes in a tree model where the stresses are summed up. The tree (including the stress distributions) is exactly the same as in Fig. 5. Quantities are plotted in arbitrary units.

simulations with the sum rule. On first glance, one would expect that the tree model behaves the same whether we choose Eq. (2) or Eq. (3) for calculating the effective stress on the agents, at least for exponential stress, because of Eq. (9). However, this is not exactly the case. In Fig. 11, we display the distribution of event sizes in a simulation where stresses are summed up. The tree used in this simulation is exactly the same we used in the simulation of Fig. 5. This allows an easy comparison between the two choices for  $\mathcal{A}$ . Note that all stress distributions are exponentials, which implies that Eq. (9) holds. We observe the emergence of a power-law decrease, similar to the situation with the maximum rule. However, the resulting distribution is slightly steeper than in Fig. 5, with an exponent of  $2.6 \pm 0.1$ . This steeper distribution shows that the conception of a tree being equivalent to an ensemble of coherent-noise models is less accurate when stresses are summed up. Second-order effects arise because all stress distributions contribute to the overall system's behavior at all times (which is in contrast to the case when we use the maximum of the stresses). Consequently, the agents feel the stress less coherently, resulting in a smaller number of large events.

## VII. CONCLUSIONS

Coherent-noise models have been proposed by Newman and Sneppen to explain the occurrence of power laws in a number of natural systems. The underlying mechanism is remarkably simple and robust. However, the coherent stress necessary to make these models work is an impediment to their application, since in most systems coherence is not present *a priori*, and local phenomena are important. In this paper, we were able to show that in hierarchical contexts, coherence can arise naturally in large subsystems. In the tree models we presented, the system breaks down into a number of subsystems, each of them having a high degree of coherence and being largely independent of the rest. Interestingly, the number of subsystems of size  $k$  decreases as  $k^{-2}$  for a large class of different trees. The emergence of coherent subsystems is closely connected to the domination of some stress distributions by others. We should always observe this phenomenon if the function  $\mathcal{A}$  is proportional to a single stress distribution in the limit of large stresses.

We made also an interesting observation about the agents lifetimes. We found the distribution of lifetimes to be the same in the tree model and in coherent-noise models, as long as the stress distributions in both models have the same functional dependency. Furthermore, from the arguments given in Sec. VIC we can deduce an even more general statement. In any system where agents under the influence of stress are modeled as in coherent-noise systems, the distribution of the agents' lifetimes will be a power law, even if there is no correlation between stresses different agents feel. This is a new explanation for the appearance of power-law distributed lifetimes or waiting times in nonequilibrium systems valid under extremely weak conditions.

Further work extending the tree model presented here could address appearance and disappearance of agents. If we consider, for example, the case of biological evolution and extinction, the biodiversity is constantly changing, with the main tendency of exponential growth throughout the past

1000 million years [15] (this trend, however, has changed dramatically recently, because of ever increasing human activity [16]). "Real" extinction and speciation could be incorporated into the tree model by removing from the tree the agents hit by stress, as it has been done already in the case of coherent-noise models [4]. Related to this, one could consider trees changing their structure. Up to now, we studied only fixed trees, mainly for reasons of simplicity. Another extension could be the consideration of vector stresses, as it has been done by Sneppen and Newman for the original coherent-noise model [13], inspired by a similar generalization of the Bak-Sneppen model [17].

#### ACKNOWLEDGMENTS

We thank Thomas Daube for useful comments at an early stage of the manuscript and Xavier Gabaix for pointing us to a simplified calculation of the effective stress distribution.

- 
- [1] M. E. J. Newman and K. Sneppen, *Phys. Rev. E* **54**, 6226 (1996).
- [2] M. E. J. Newman, *Proc. R. Soc. London, Ser. B* **263**, 1605 (1996).
- [3] M. E. J. Newman, *J. Theor. Biol.* **189**, 235 (1998).
- [4] C. Wilke and T. Martinetz, *Phys. Rev. E* **56**, 7128 (1997).
- [5] L. W. Alvarez, *Phys. Today* **50** (7), 24 (1987).
- [6] D. M. Raup, *Extinction: Bad Genes or Bad Luck?* (Oxford University Press, Oxford, 1993).
- [7] Y. Y. Kagan, *Physica D* **77**, 160 (1994).
- [8] C. Wilkes, S. Altmeyer, and T. Martinetz, in *Proceedings of "Artificial Life VI,"* edited by C. Adami, R. Belew, H. Kitano, and C. Taylor (MIT Press, Los Angeles, 1998).
- [9] J. S. Nicolis, *Dynamics of Hierarchical Systems: An Evolutionary Approach* (Springer, Berlin, 1986).
- [10] R. Rammal, G. Toulouse, and M. A. Virasoro, *Rev. Mod. Phys.* **58**, 765 (1986).
- [11] A. I. Olemskoi and A. D. Kiselev, physics/9802035 (unpublished).
- [12] T. E. Harris, *The Theory of Branching Processes* (Springer, Berlin, 1963).
- [13] K. Sneppen and M. E. J. Newman, *Physica D* **107**, 292 (1997).
- [14] C. Wilke, S. Altmeyer, and T. Martinetz, *Physica D* **120**, 401 (1998).
- [15] M. J. Benton, *Science* **268**, 52 (1995).
- [16] N. Myers, *Science* **278**, 597 (1997).
- [17] S. Boettcher and M. Paczuski, *Phys. Rev. Lett.* **76**, 348 (1996).